Cellular & Molecular Immunology (2017) 14, 830–841

www.nature.com/cmi

RESEARCH ARTICLE

BRD7 plays an anti-inflammatory role during early acute inflammation by inhibiting activation of the NF-κB signaling pathway

Ran Zhao[1,2,3], Yukun Liu[2,3], Heran Wang[2,3], Jing Yang[2,3], Weihong Niu[2,3], Songqing Fan[4], Wei Xiong[2,3], Jian Ma[2,3], Xiaoling Li[2,3], Joshua B Phillips[5], Ming Tan[5], Yuanzheng Qiu[1], Guiyuan Li[2,3] and Ming Zhou[1,2,3]

Increasing evidence has shown a strong association between tumor-suppressor genes and inflammation. However, the role of BRD7 as a novel tumor suppressor in inflammation remains unknown. In this study, by observing BRD7 knockout mice for 6–12 months, we discovered that compared with BRD7$^{+/+}$ mice, BRD7$^{-/-}$ mice were more prone to inflammation, such as external inflammation and abdominal abscess. By using mouse embryo fibroblast (MEF) cells from the BRD7 knockout mouse, an *in vitro* lipopolysaccharide (LPS)-stimulated MEF cell line was established. The mRNA levels of interleukin-6 (IL-6), tumor necrosis factor-α (TNF-α), chemokine (C-X-C motif) ligand 1 (CXCL-1) and inducible nitric oxide synthase (iNOS) were significantly increased in BRD7$^{-/-}$ MEF cells compared with BRD7$^{+/+}$ MEF cells after LPS stimulation for 1 or 6 h. In addition, the cytoplasm-to-nucleus translocation of nuclear factor kappa-B (NF-κB; p65) and an increased NF-κB reporter activity were observed in BRD7$^{-/-}$ MEF cells at the 1 h time point but not at the 6 h time point. Furthermore, an *in vivo* dextran sodium sulfate (DSS)-induced acute colitis model was created. As expected, the disease activity index (DAI) value was significantly increased in the BRD7$^{-/-}$ mice after DSS treatment for 1–5 days, which was demonstrated by the presence of a significantly shorter colon, splenomegaly and tissue damage. Moreover, higher expression levels of IL-6, TNF-α, p65, CXCL-1 and iNOS, and an increased level of NF-κB (p65) nuclear translocation were also found in the DSS-treated BRD7$^{-/-}$ mice. These findings suggest that BRD7 has an anti-inflammatory role during early acute inflammation by inhibiting activation of the NF-κB signaling pathway, which provides evidence to aid in understanding the therapeutic effects of BRD7 on inflammatory diseases.
Cellular & Molecular Immunology (2017) **14,** 830–841; doi:10.1038/cmi.2016.31; published online 4 July 2016

Keywords: acute inflammation; BRD7; DSS; LPS; NF-κB pathway

INTRODUCTION

The gene encoding bromodomain-containing protein 7 (BRD7), which was cloned in our laboratory using complementary DNA (cDNA) representational difference analysis, has been identified as a tumor-suppressor gene in multiple cancers, such as nasopharyngeal carcinoma, osteosarcoma, ovarian carcinoma and breast cancer. It has been found to inhibit the cell cycle G1–S phase progression, initiate apoptosis and reverse cellular malignancy through the ras/MEK/ERK, Rb/E2F and Wnt signaling pathways.[1–4] BRD7 is a member of the bromodomain family, which includes BRD2, BRD3, BRD9 and BRDT,[5–7] and can recognize and bind to acetylated histone H3.[8] BRD7 is primarily localized in the nucleus and possesses a functional nuclear localization signal sequence.[9] It has been identified as a subunit of the SWItch/Sucrose Non-Fermentable (SWI/SNF) chromatin-remodeling complexes, is involved in transcriptional regulation as a transcription factor[10] and

[1]Xiangya Hospital, Central South University, Changsha, Hunan 410008, China; [2]Cancer Research Institute, Central South University, Changsha, Hunan 410078, China; [3]Key Laboratory of Carcinogenesis and Ministry of Health and Key Laboratory of Carcinogenesis and Cancer Invasion, Ministry of Education, Changsha, Hunan 410078, China; [4]The Second Xiangya Hospital, Central South University, Changsha, Hunan 410011, China and [5]Mitchell Cancer Institute, University of South Alabama, Mobile, AL 36604, USA
Correspondence: M Zhou, PhD, Cancer Research Institute, Central South University, Key Laboratory of Carcinogenesis, Ministry of Health, Key Laboratory of Carcinogenesis and Cancer Invasion, Ministry of Education, 110 Xiangya Road, Changsha, Hunan 410078, China.
E-mail: zhouming2001@163.com
Received: 24 November 2015; Revised: 6 May 2016; Accepted: 6 May 2016

has a critical role in cellular growth, cell cycle progression, signal-dependent gene expression and tumor development.

Increasing evidence shows that inflammation has critical roles in tumor suppression or promotion,[11–13] and many tumor-suppressor genes, such as *PTEN*,[14] *p53*[15] and *PDCD4*,[16] participate in immune responses, inflammatory diseases and other physiological and pathological processes. Our previous studies have demonstrated that BRD7 functions as a tumor suppressor in nasopharyngeal carcinoma.[1] However, the precise role of BRD7 in inflammation has not yet been investigated. In this study, we first constructed lipopolysaccharide (LPS)-stimulated mouse embryo fibroblast (MEF) cells and a dextran sodium sulfate (DSS)-induced acute colitis mouse model by using BRD7 knockout mice and investigated the function of BRD7 and its molecular mechanism in inflammation using these models. We found that $BRD7^{-/-}$ mice and $BRD7^{-/-}$ MEF cells were more susceptible to inflammation than the $BRD7^{+/+}$ controls. We also found that the mRNA and protein levels of interleukin-6 (IL-6), tumor necrosis factor-a (TNF-α), chemokine (C-X-C motif) ligand 1 (CXCL-1) and inducible nitric oxide synthase (iNOS) were significantly increased after the treatment with LPS or DSS, and this was followed by the nuclear translocation of nuclear factor kappa-B (NF-κB; p65) and activation of the NF-κB pathway, which suggested that BRD7 deficiency promoted early acute inflammation both *in vitro* and *in vivo*. These findings suggest that the anti-inflammatory properties of BRD7 might result from the inhibition of IL-6, TNF-α, CXCL-1 and iNOS expression by preventing the activation of the NF-κB signaling pathway during early acute inflammation. Together, these results provide evidence for the therapeutic utility of BRD7 in inflammatory diseases.

MATERIALS AND METHODS

Mice and animal care

BRD7 knockout mice were generated to allow both conditional and global disruption of the *BRD7* gene by using the Cre/loxp recombination system to target exons 3 and 4 of BRD7 in a C57BL/6 background in our study, which was detailed in our previous publication.[17–18] The genotypes were further confirmed using western blot and PCR assays. The mice were raised with a 12-h light/dark schedule under specific pathogen-free conditions. This study was conducted in strict accordance with the recommendations of the Guide for the Care and Use of Laboratory Animals (National Institutes of Health). The protocol was approved by the Animal Ethics Committee of Central South University.

Preparation of mouse embryonic fibroblasts

Heterozygous BRD7 mice were killed by cervical dislocation during pregnancy day 14–15 and were cleaned using 75% alcohol. The uteri were removed and flushed with phosphate-buffered saline (PBS). MEF cells were then prepared according to a previously described method.[19] Briefly, the heads and internal organs were removed, and the embryos were minced in Hanks' balanced salt solution using two surgical knives. The minced tissue fragments were suspended in a 0.25% trypsin-EDTA solution and agitated for 30 min in a 37 °C cell incubator. The trypsin digests were transferred to DMEM supplemented with 10% fetal bovine serum (FBS), and the floating cells were collected. The suspensions of collected cells were centrifuged at 1000*g* for 10 min, and the pelleted cells were suspended in DMEM supplemented with 10% FBS and cultured at 37 °C in 5% CO_2. The next day, the culture medium was replaced with fresh medium and the cells were cultured for three more days. The confluent cells were then trypsinized and stored under liquid nitrogen until use.

LPS-stimulated MEF cells

MEF cells that expressed or did not express BRD7 were stimulated with 1 μg/ml LPS (*Escherichia coli*: Serotype O55: B5; Sigma-Aldrich, St Louis, MO, USA) for 0, 1 or 6 h, after which the cells were collected using a cell scraper and used for gene and protein expression analyses.

RNA extraction, real-time PCR and RT-PCR

The total RNA was extracted from the cultured cells using TRIzol (Invitrogen, Carlsbad, CA, USA). The cDNA was synthesized from the total RNA using a Reverse Transcription System (Fermentas, Glen Burnie, MD, USA) according to the manufacturer's instructions. GAPDH was amplified in parallel as an internal control. The expression level of each gene was quantified by measuring the cycle threshold (Ct) values and normalized relative to that of GAPDH using the 2-ΔΔCt method. The primers used in the reaction were as follows: mouse IL-6 (forward, 5′-CCTCTCTGCAAGAGACTTCCA TCCA-3′; reverse, 5′-AGCCTCCGACTTGTGAAGTGGT-3′), mouse TNF-α (forward, 5′-AGGGGCCACCACGCTCTTCT-3′; reverse, 5′-CATGCCGTTGGCCAGGAGGG-3′), mouse iNOS (forward, 5′-CCTGGTACGGGCATTGCT-3′; reverse, 5′-CGGC ACCCAAACACCAA-3′), mouse CXCL-1 (forward, 5′-GCCA CCCGCTCGCTTCTCTG-3′; reverse, 5′-CAAGGCAAGCCTC GCGACCA-3′), mouse IL-10 (forward, 5′-AGTTCAGAGCT CCTAAGAGAGTTGTGA-3′; reverse, 5′-CCTCTGAGCTGCT GCAGGAA-3′), mouse MCP-1 (forward, 5′-TCTGGGCCTG CTGTTCACA-3′; reverse, 5′-CCTACTCATTGGGATCATCT TGCT-3′) and mouse GAPDH (forward, 5′-TCTGACGT GCCGCCTGGAGA-3′; reverse, 5′-CAGCCCCGGCATCGAA GGTG-3′). PCR was performed using PCR Mix (BioTeKe, Beijing, China). The PCR products were analyzed after electrophoresis in a 1% agarose gel at 120 V for 15 min.

Immunofluorescence assay

The immunofluorescence assay for NF-κB nuclear translocation was performed according to a previously described method.[20] Cells or sections of colon were incubated with a rabbit monoclonal anti-p65 antibody (Santa Cruz Biotechnology, Paso Robles, CA, USA) overnight at 4 °C. The samples were then immunostained with an Alexa Fluor 488-conjugated anti-rabbit IgG (Life Technology, Carlsbad, CA, USA) for 1 h at 37 °C. The samples were then washed and mounted in medium containing 4',6-diamidino-2-phenylindole (DAPI) to

counterstain the nuclei, after which they were imaged using a confocal laser-scanning microscope (UltraView, Perkin Elmer, Cambridge, UK).

Gene transfection

BRD7$^{-/-}$ MEF cells were transfected with the pIRES Neo2 Flag/BRD7 plasmid in medium free of FBS and antibiotics using Lipofectamine 2000 (Invitrogen) according to the manufacturer's instructions. MEF cells transfected with the pIRES Neo2 plasmid were used as controls. The medium was changed 5 h after transfection. The cells were grown for a total of 24 h before use in the experiments.

Western blot analysis

MEF cells were exposed to various experimental conditions for the indicated times (LPS stimulation) before being harvested and lysed for protein extraction using sodium dodecyl sulfate (Sigma-Aldrich) supplemented with phosphatase and protease inhibitors (Roche, Mannheim, Germany). The protein concentrations were determined using the Bio-Rad Protein Assay Kit (Bio-Rad, Hercules, CA, USA). After centrifugation at 15 000*g* for 15 min, 80 μg of the supernatants was separated by sodium dodecyl sulfate-polyacrylamide gel electrophoresis and transferred to polyvinylidene fluoride membranes (Millipore, Billerica, MA, USA). The membranes were blocked with 5% nonfat milk in Tris-buffered saline/Tween 20 (25 mM Tris-HCl, 150 mM NaCl, pH 7.5 and 0.05% Tween 20) and then were incubated overnight at 4 °C with primary antibodies directed against the following: p65 (Santa Cruz Biotechnology), p-p65 (Beyotime, Beijing, China), IkB-α (Beyotime), BRD7 (Proteintech, Wuhan, China), Flag (Sigma-Aldrich), IL-6 (Proteintech), β-actin (Santa Cruz Biotechnology) and GAPDH (Santa Cruz Biotechnology). After washing with Tris-buffered saline/Tween 20, the membranes were incubated with horseradish peroxidase (HRP)-conjugated secondary antibodies and were visualized using the electrochemiluminescence detection system.

Luciferase reporter assay

We inserted the consensus sequence of the downstream NF-κB target genes into the pGL3-Basic reporter vector (Promega, Madison, WI, USA) to create an NF-κB luciferase reporter construct. The cells were co-transfected with 1 μg of the NF-κB luciferase reporter construct and 0.1 μg of a *Renilla* luciferase-expressing plasmid (pRL-TK; Promega) using jetPRIME (Polyplus Transfection). Twenty-four hours after transfection, the cells were treated with LPS (1 μg/ml) for 0, 1 or 6 h. The cells were harvested and lysed, and the levels of firefly luciferase and *Renilla* luciferase activity were determined using a luciferase assay system (Dual-Glo; Promega). For each lysate, the level of firefly luciferase activity was normalized to that of the *Renilla* luciferase activity to assess the transfection efficiencies.

DSS-induced early acute colitis

Acute colitis was induced by administering DSS in the drinking water. Male and female mice that were 8–12 weeks of age were provided *ad libitum* access to a solution of 2% DSS (MP Biomedicals, Solon, OH, USA; molecular weight 36–50 kDa) by the oral intake of drinking water for 6 days (BRD7$^{+/+}$ group, $n=25$; BRD7$^{-/-}$ group, $n=21$). The mice were weighed and visually inspected for diarrhea and rectal bleeding each day.[21] Five mice that were randomly selected from each group were sequentially killed on day 4. The colon, from the ileocecal junction to the anus, was removed from each animal and flushed with cold PBS. Colon tissue obtained from each mouse was processed for histological, immunohistochemical and immunofluorescence assays.

Disease activity index

Clinical assessment of inflammation included daily monitoring of body weight, stool consistency and fecal blood. The disease activity index (DAI) was calculated according to a modified protocol by grading weight loss on a scale of 0–4 (0 = normal; 1 = 1–5%; 2 = 5–10%; 3 = 10–20%; 4 ⩾ 20%), stool consistency on a scale of 0–2 (0 = normal; 1 = loose stools; 2 = diarrhea) and the presence of fecal blood on a scale of 0–2 (0 = normal; 1 = bleeding; 2 = severe bleeding). The final DAI value for each animal was expressed as the average of the combined scores.[22]

Cytokine quantification by enzyme-linked immunoassay

Peritoneal fluid was collected from the mice in each group, and the protein level was measured using a mouse IL-6 enzyme-linked immunoassay (ELISA) kit and a mouse TNF-α ELISA kit (BD Pharmingen, San Jose, CA, USA) according to the manufacturers' recommendations.

Histology and immunohistochemistry

Colons were collected for histological analysis. Tissues were embedded in paraffin and cut into 4-μm-thick sections. Sections from each sample were stained using hematoxylin and eosin (H&E). To assess the expression of IL-6, TNF-α, CXCL-1, iNOS and p65 in the colon tissues, 4-μm-thick sections were incubated with an antibody directed against NF-κB (p65; 1:100 dilution) overnight at 4 °C, and then incubated with a HRP-conjugated secondary antibody at room temperature for 1 h, after which they were then reacted with 3,3'-diaminobenzidine (Maixin, Fujian, China), and the nuclei were counterstained with hematoxylin. Morphometric analyses of the colon tissues were performed using an Olympus BX51 microscope (Olympus, Tokyo, Japan).

Data analysis

The data obtained in this study are expressed as the mean values ± s.d. from at least three independent experiments using triplicate samples for the individual treatments. Statistical analyses were performed using two-way ANOVA or Fisher's exact test (Prism 6, GraphPad Software, San Diego, CA, USA). A *P*-value of <0.05 was considered statistically significant.

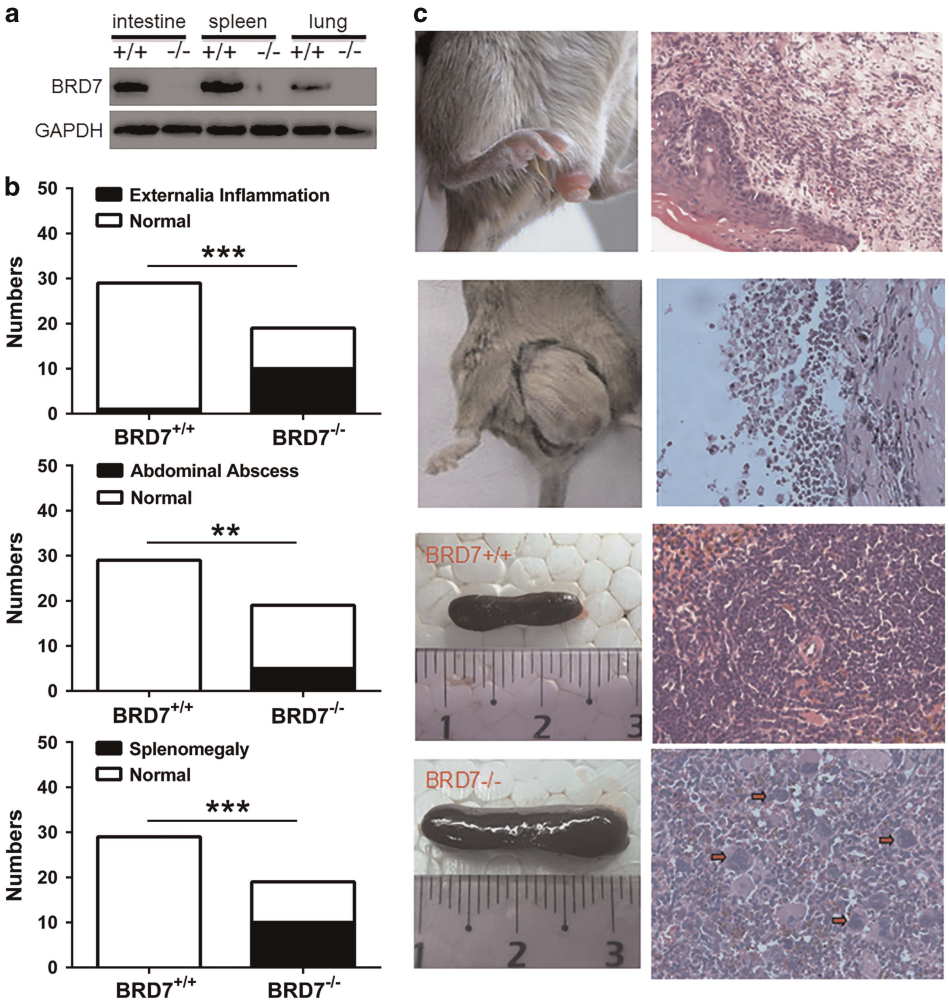

Figure 1 BRD7$^{-/-}$ mice are more susceptible to surface inflammation. (**a**) Genotype identification of BRD7 knockout mice. The three types of representative tissues (intestine, spleen and lung) were obtained from BRD7$^{+/+}$ and BRD7$^{-/-}$ mice, and the expression of BRD7 was detected by western blotting using an antibody specific for BRD7. (**b**) The number of animals with external inflammation (the upper), abdominal abscess (the middle) and splenomegaly (the lower) in BRD7$^{-/-}$ and BRD7$^{+/+}$ mice. (**c**) Representative images of the external inflammation, abdominal abscess and splenomegaly inflammation sites in BRD7$^{-/-}$ mice (left). Representative H&E-stained sections from BRD7$^{-/-}$ inflammation mice (right; all pictures at a ×100 magnification except for the BRD7$^{-/-}$ splenomegaly magnification of ×200). Arrows indicate megakaryocytes and coenocytes cells. BRD7, bromodomain-containing protein 7; H&E, hematoxylin and eosin. The data are expressed as the mean values±s.d. $^{**}P<0.01$, $^{***}P<0.001$.

RESULTS

BRD7$^{-/-}$ mice are susceptible to inflammation

To investigate the role of BRD7 in the occurrence of inflammation, the BRD7 knockout mice generated by our group were raised in the general environment. Routine genotyping of these mice was conducted using western blotting (Figure 1a). A single immunoreactive band migrating at the size expected for the BRD7 protein was detected in the intestine, spleen and lung from BRD7$^{+/+}$ mice, whereas no BRD7 protein was detected in BRD7$^{-/-}$ mice. During 6–12 months of observation, we found that the BRD7$^{-/-}$ mice were more susceptible to inflammation than the BRD7$^{+/+}$ mice. Among 19 BRD7$^{-/-}$ mice, 10 developed external inflammation, 5 developed abdominal abscesses (5/19) and 9 presented splenomegaly (9/19). Among 29 BRD7$^{+/+}$ mice, only one mouse displayed external inflammation (1/29) and none of them displayed an abdominal abscess or splenomegaly (0/29; Figure 1b). Figure 1c shows representative images of the inflammation in the BRD7$^{-/-}$ mice. The severity of the inflammation in the BRD7$^{-/-}$ mice was also histologically examined using H&E staining. Compared with the BRD7$^{+/+}$ mice, the inflamed tissues of the BRD7$^{-/-}$ mice exhibited extensive inflammatory cell infiltration and their spleens were also characterized by the presence of megakaryocytes and coenocytes, accompanied by erythrocytolysis (Figure 1c). These results demonstrated that the BRD7$^{-/-}$ mice are susceptible to inflammation.

BRD7 deficiency promotes LPS-induced early inflammatory responses in MEF cells

To examine the effects of BRD7 deficiency on inflammatory responses, MEF cells isolated from BRD7$^{+/+}$, BRD7$^{+/-}$ and

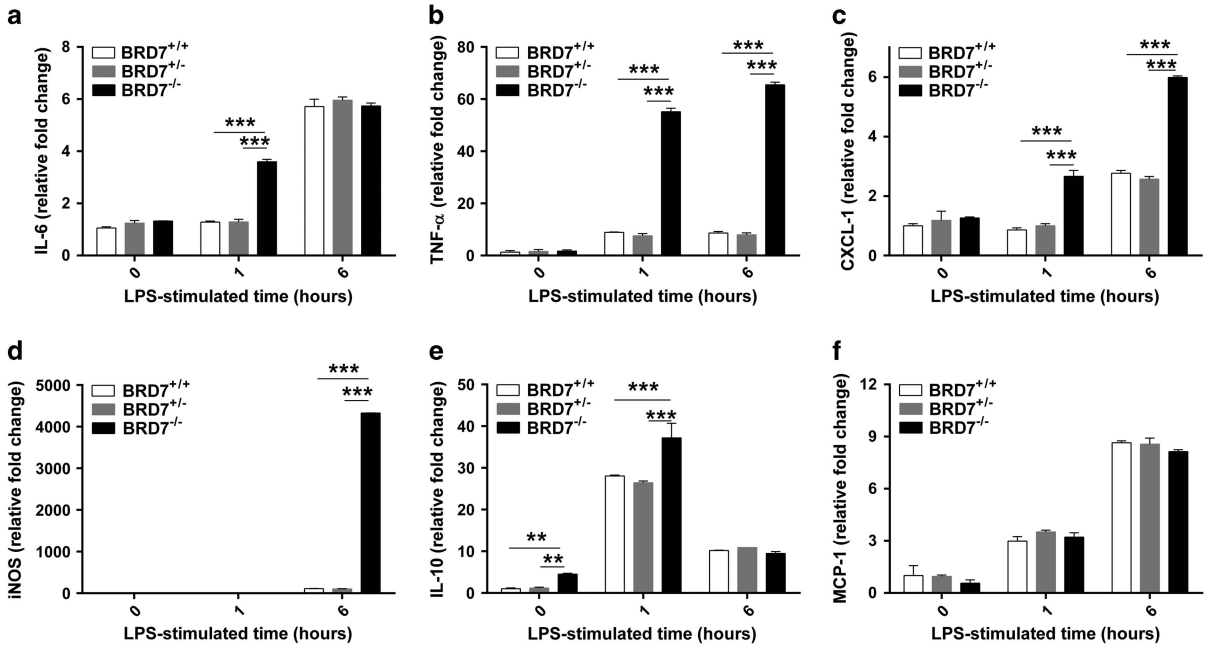

Figure 2 BRD7 deficiency promotes LPS-induced early inflammatory responses in MEF cells. (**a–f**) The mRNA levels of IL-6, TNF-α, CXCL-1, iNOS, IL-10 and MCP-1 in MEF cells stimulated with LPS for 0, 1 or 6 h were determined using qPCR. The results are representative of three independent experiments and were expressed as the mean values ± s.d. $^{**}P<0.01$, $^{***}P<0.001$ compared with the $BRD7^{+/+}$ control. BRD7, bromodomain-containing protein 7; LPS, lipopolysaccharide; MEF, mouse embryo fibroblast; qPCR; quantitative polymerase chain reaction.

$BRD7^{-/-}$ mice were stimulated with LPS for 0, 1 or 6 h. Subsequently, the expression levels of some of the key inflammatory cytokines involved in inflammation-related diseases, such as IL-6, TNF-α, IL-10, CXCL-1, MCP-1 and pro-inflammatory enzyme iNOS, were examined. As expected, all of these inflammatory mediators were expressed at low levels in $BRD7^{+/+}$, $BRD7^{+/-}$ and $BRD7^{-/-}$ MEF cells under basal conditions. The expression levels of IL-6 and CXCL-1 showed a tendency to increase in $BRD7^{-/-}$ MEF cells compared with $BRD7^{+/+}$ and $BRD7^{+/-}$ MEF cells. However, the mRNA levels of all of these inflammatory mediators were upregulated in the three groups after stimulation with LPS, whereas the mRNA levels of the pro-inflammatory mediators, including IL-6, TNF-α, CXCL-1 and iNOS, were higher in $BRD7^{-/-}$ mice than those in the $BRD7^{+/+}$ and $BRD7^{+/-}$ groups after LPS stimulation for 1 or 6 h (Figures 2a–d). The expression of MCP-1 mRNA in MEF cells was not significantly altered by BRD7 deficiency (Figure 2f). Unexpectedly, the expression level of the anti-inflammatory factor IL-10 was also higher in $BRD7^{-/-}$ MEF cells than in the $BRD7^{+/+}$ and $BRD7^{+/-}$ groups (Figure 2e), which may have resulted from an inflammation-induced compensatory increase in anti-inflammatory factors. No difference in the expression level of IL-10 was found in $BRD7^{+/+}$ and $BRD7^{+/-}$ groups. Thus, we only focused on the investigation of the $BRD7^{+/+}$ and $BRD7^{-/-}$ groups in the next study (Supplementary Figure S1). All of these results suggested that BRD7 deficiency leads to the upregulated expression of IL-6, TNF-α, CXCL-1 and iNOS in LPS-stimulated MEF cells and promotes LPS-induced early inflammation.

BRD7 deficiency enhances LPS-induced NF-κB activation

As BRD7 deficiency led to the upregulation of IL-6, TNF-α, CXCL-1 and iNOS expression in LPS-stimulated MEF cells, all of which are downstream targets of NF-κB, we evaluated the effect of BRD7 deficiency on LPS-induced NF-κB activation. As expected, the subcellular localization of p65 was in the cytoplasm in both $BRD7^{+/+}$ and $BRD7^{-/-}$ MEF cells in the inactive state before LPS stimulation (Figure 3a). However, an obvious p65 translocation from the cytoplasm to the nucleus was found in $BRD7^{-/-}$ MEF cells after LPS stimulation for 1 h, but p65 returned to the cytoplasm after LPS stimulation for 6 h (Figure 3a). There were no obvious changes observed in the $BRD7^{+/+}$ MEF cells at the 1-h time point after LPS stimulation, but little p65 nuclear translocation from the cytoplasm was observed after LPS stimulation at 6 h. Next, we examined the expression levels of p65, p-p65 and IκB-α from the lysates of MEF cells stimulated with LPS. As expected, the total protein levels of p65 were not changed by LPS stimulation in either the $BRD7^{+/+}$ or the $BRD7^{-/-}$ MEF cells (Figures 3b and c). However, an obviously increased level of p-p65 expression and a decreased level of IkB-α expression were observed in $BRD7^{-/-}$ MEF cells after 1 h of LPS stimulation, and a slight increase in p-p65 expression and a decreased level of IkB-α expression were observed in the $BRD7^{+/+}$ MEF cells after 6 h of LPS stimulation (Figures 3b and c), which is consistent with

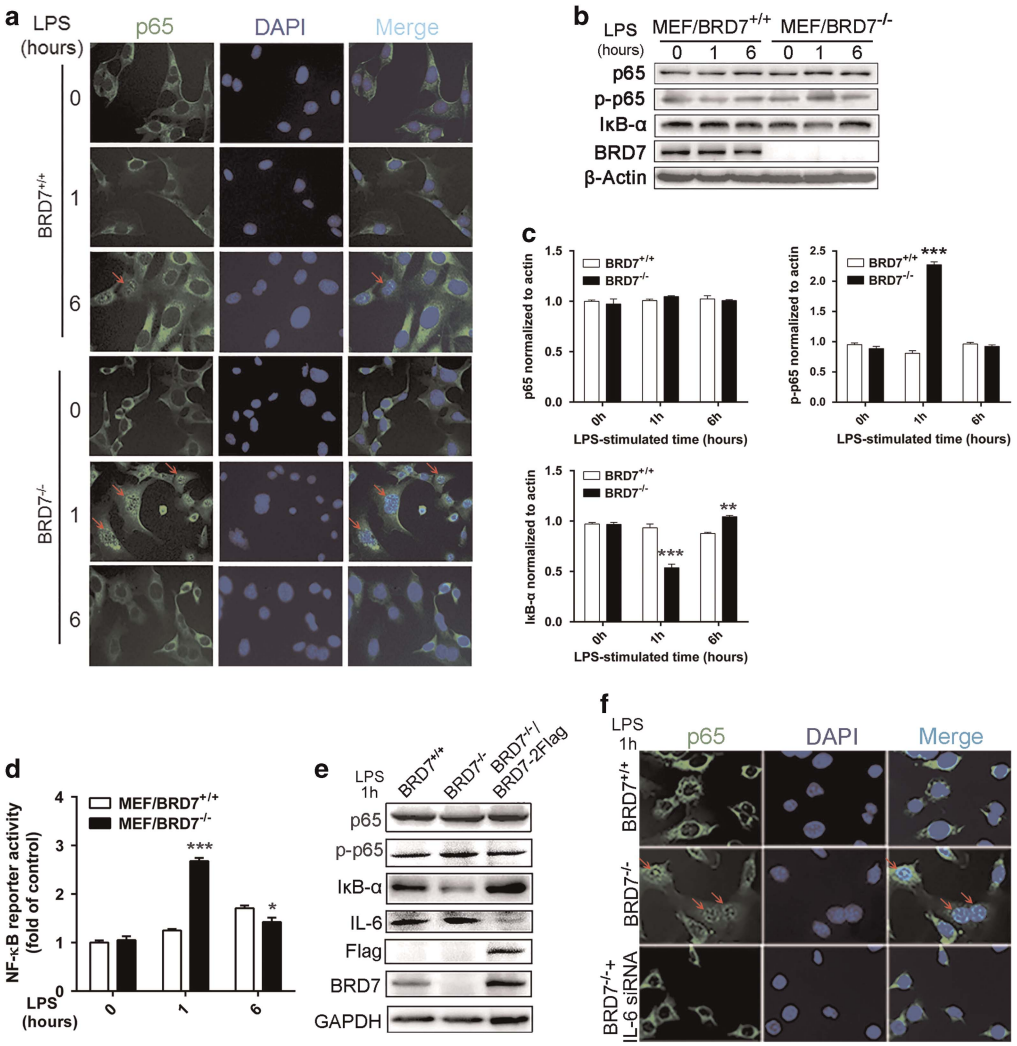

Figure 3 BRD7 deficiency promotes the activation of NF-κB signaling pathways and the transcriptional regulation of NF-κB-mediated downstream target genes in LPS-induced inflammation. (**a**) Immunofluorescence was performed to analyze NF-κB p65 nuclear translocation after stimulation with LPS for 0, 1 or 6 h in MEF cells. Arrows indicate p65 nuclear translocation from the cytoplasm in the cells. (**b**) The levels of p65, p-p65, IκB-α and BRD7 in MEF cells were determined by western blotting after 0, 1 or 6 h of LPS stimulation. (**c**) Densitometric analysis was performed to determine the relative ratios of each protein normalized to the level of β-actin. The results are representative of three independent experiments and are expressed as the mean values ± s.d. $^{**}P<0.01$, $^{***}P<0.001$ compared with $BRD7^{+/+}$ MEF cells after 0 h of LPS stimulation. (**d**) Levels of NF-κB luciferase activity in MEF cells after 0, 1 or 6 h of LPS stimulation, determined by a luciferase reporter assay. The results are representative of three independent experiments and are expressed as the mean values ± s.d. $^{*}P<0.05$, $^{***}P<0.001$ compared with the $BRD7^{+/+}$ control. (**e**) The levels of p65, p-p65, IκB-α, IL-6, Flag and BRD7 expression in $BRD7^{-/-}$ MEF cells that were transiently transfected with pIRES Neo/BRD7-Flag for 24 h and then stimulated with LPS for 1 h were determined using western blotting. (**f**) Immunofluorescence was performed to examine NF-κB p65 translocation after stimulation with LPS for 1 h in $BRD7^{+/+}$, $BRD7^{-/-}$ and $BRD7^{-/-}$ IL-6 siRNA-transfected MEF cells. Arrows indicate p65 translocation in the cells. BRD7, bromodomain-containing protein 7; LPS, lipopolysaccharide; MEF, mouse embryo fibroblast; NF-kB, nuclear factor kappa-B; siRNA, short interfering RNA.

the results of the p65 cytoplasm-to-nucleus translocation assay (Figure 3a).

Because NF-κB is the central regulator of the inflammatory responses to LPS, the consensus sequences of NF-κB downstream target genes were inserted into the pGL3-Basic luciferase reporter vector to further determine the role of the BRD7 in mediating NF-κB-induced cytokine/chemokine expression. The luciferase activity was determined using a dual luciferase reporter assay system after treatment with 1 μg/ml of LPS for 0, 1 or 6 h. As expected, the BRD7 deficiency promoted the transcriptional activation of NF-κB after 1 h of LPS stimulation, whereas recovery was observed at 6 h (Figure 3d), which is consistent with the above results.

To extend our observations, we further examined the effect of restoring BRD7 expression in $BRD7^{-/-}$ MEF cells on the activation of NF-κB following LPS stimulation for 1 h. Moreover, IL-6 was also examined, as it is the key factor involved in inflammation-related diseases. As shown in Figure 3e, the total protein level of p65 was not changed by LPS stimulation in $BRD7^{+/+}$, $BRD7^{-/-}$ or $BRD7^{-/-}$ BRD7-

2Flag-expression plasmid-transfected MEF cells. However, recovered expression of IL-6, p-p65 and IkB-α was found in BRD7$^{-/-}$ MEF cells transiently transfected with BRD7-2Flag compared with the BRD7$^{-/-}$ MEF cells after LPS stimulation for 1 h (Figure 3e), which supports the hypothesis that BRD7 has a critical role in LPS-induced early acute inflammation. Meanwhile, Bay11-7082 (Selleckchem), the inhibitor of NF-kB, was used to prevent the activation of NF-kB. The down-regulated expressions of IL-6, TNF-α and CXCL-1 were found in LPS-stimulated BRD7$^{-/-}$ MEF cells (Supplementary Figure S2). Conversely, we further examined the subcellular localization of p65 in BRD7$^{+/+}$, BRD7$^{-/-}$ and IL-6 short interfering RNA (siRNA)-transfected BRD7$^{-/-}$ (for blocking of IL-6) MEF cells after LPS stimulation for 1 h (Supplementary Figure S3 and Figure 3f). The obvious translocation of p65 from the nucleus to the cytoplasm was found in BRD7$^{-/-}$ MEF cells transfected with IL-6 siRNA (Figure 3f). The above-mentioned results suggested that BRD7 deficiency enhances the expression of pro-inflammatory mediators, such as IL-6, TNF-α, CXCL-1 and iNOS, in MEF cells stimulated with LPS by activating the NF-kB pathway.

Knockout of BRD7 enhances DSS-induced early acute colonic inflammation

To investigate the role of BRD7 in acute colonic inflammation, BRD7$^{+/+}$ and BRD7$^{-/-}$ mice were treated with DSS as described in the Materials and methods. As expected, DSS treatment induced inflammation effects in the large intestines of these mice. However, BRD7$^{-/-}$ mice treated with DSS showed a progressive and significant increase in the DAI value compared with the BRD7$^{+/+}$ mice from day 1 to 5 ($P<0.001$), with the greatest difference observed on day 4, whereas no large difference was observed on day 6 (Figure 4a). These results indicated that BRD7 deficiency promoted DSS-induced early acute colitis. Next, colon shortening was utilized as an indicator of the disease severity in the BRD7$^{+/+}$ and BRD7$^{-/-}$ mice. Consistent with the DAI results, the colons from BRD7$^{-/-}$ mice were obviously shorter than those from the BRD7$^{+/+}$ mice after 4 days of DSS treatment (Figures 4b and c). Moreover, the BRD7$^{-/-}$ mice exhibited a significant increase in the weight of their spleens, indicating that BRD7 deficiency promoted DSS-induced splenomegaly (Figures 4b and c).

The severity of the colonic inflammation and ulceration was further evaluated by histopathological analysis using H&E staining after DSS treatment for 4 or 6 days. On day 4, the DSS-induced mucosal damage was characterized by gross ulceration, accompanied by extensive infiltration of granulocytes and mononuclear cells into the mucosa, as well as by congestion and edema of the submucosa. Strikingly, there was significant tissue damage in the DSS-treated BRD7$^{-/-}$ mice, which included the pronounced infiltration of inflammatory cells into the mucous layer, epithelial erosion, loss of the normal crypt architecture and crypt abscesses (Figure 4d). These effects were largely prevented by the presence of BRD7,

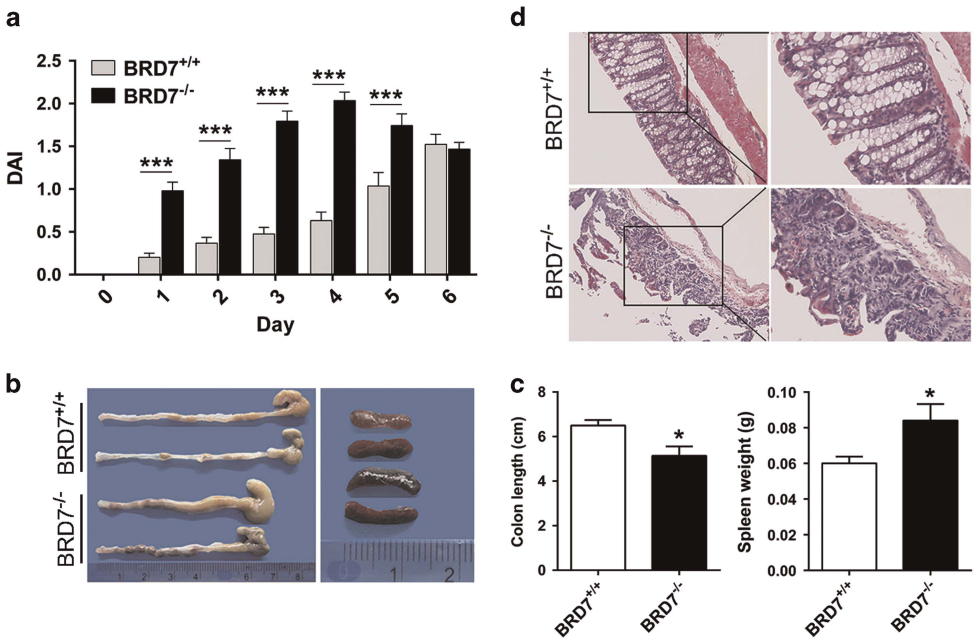

Figure 4 Knockout of BRD7 enhances DSS-induced early acute colonic inflammation. BRD7$^{+/+}$ and BRD7$^{-/-}$ mice received 2% DSS for 6 days. (**a**) Changes in the DAI values of the mice during the induction of colitis. (**b**) Macroscopic appearances of colons and spleens collected from each group of mice during the disease process. (**c**) The colon lengths and spleen weights of each group of mice were measured and are displayed in the bar graphs. (**d**) Representative H&E-stained sections of colons from BRD7$^{+/+}$ and BRD7$^{-/-}$ mice at 4 days following DSS treatment (left, ×100 magnification; right, ×200 magnification). The results presented are the mean values ± s.d. Differences between the groups were evaluated using ANOVA (BRD7$^{+/+}$ group, $n=25$; BRD7$^{-/-}$ group, $n=21$). *$P<0.05$, ***$P<0.001$ compared with the BRD7$^{+/+}$ mice with DSS-induced colitis. ANOVA, analysis of variance; BRD7, bromodomain-containing protein 7; DAI, disease activity index; DSS, dextran sodium sulfate; H&E, hematoxylin and eosin.

as DSS-treated BRD7$^{+/+}$ mice exhibited less inflammatory cell infiltration and an intact colonic architecture with no apparent ulceration (Figure 4d). In addition, BRD7 significantly attenuated the occurrence of inflammation-induced bloody stools, splenomegaly and shortening of the colon. As expected, no obvious difference was found in the degree of inflammation between the BRD7$^{+/+}$ and BRD7$^{-/-}$ groups on day 6; however, the severity of the colonic inflammation from day 6 mice was obviously reduced compared with day-4 mice following DSS treatment in both BRD7$^{+/+}$ and BRD7$^{-/-}$ groups (Supplementary Figure S4). These results demonstrated that BRD7 is required to prevent early acute inflammation in the large intestine.

BRD7 deficiency promotes the production of inflammatory mediators in DSS-induced early acute colitis

Increased pro-inflammatory cytokine production is a hallmark of DSS-induced colitis. Therefore, we investigated the effect of BRD7 on the production of inflammatory mediators in the DSS-induced early acute colitis model. The expression and secretion of the inflammatory markers IL-6 and TNF-α were evaluated in the peritoneal fluid using ELISAs. Compared with the DSS-treated BRD7$^{+/+}$ group, higher levels of IL-6 and TNF-α were detected in the DSS-treated BRD7$^{-/-}$ group (Figure 5a), supporting the hypothesis that BRD7 deficiency could significantly increase the expression and secretion of the pro-inflammatory cytokines IL-6 and TNF-α. We next evaluated the expression levels of IL-6, TNF-α, CXCL-1 and iNOS using immunohistochemical assays. As shown in Figure 5b, the DSS-treated BRD7$^{-/-}$ mice had significantly elevated levels of the inflammatory mediators IL-6, TNF-α, CXCL-1 and iNOS compared with those of the DSS-treated BRD7$^{+/+}$ group. Taken together, these data indicated that BRD7 deficiency promotes the production of inflammatory mediators in both the peritoneal fluid and colon tissues of mice with DSS-induced early acute colitis.

BRD7 deficiency promotes inflammation by activating NF-κB *in vivo*

Our *in vitro* results showed that BRD7 deficiency promoted the expression of IL-6, TNF-α, CXCL-1 and iNOS by activating the NF-κB pathway during LPS-induced early inflammatory processes (Figures 2 and 3). To extend our observations, we examined the effect of BRD7 deficiency on the activation of NF-κB *in vivo*. Our results showed that BRD7 deficiency markedly promoted the DSS-induced nuclear translocation of NF-κB (Supplementary Figure S5). In addition, nuclear and cytoplasmic proteins of colonic tissues were further extracted after DSS treatment for 4 days. The p65 protein was mainly expressed in the nucleus and rarely expressed in the cytoplasm (Figure 6a). Immunohistochemical analysis revealed that BRD7 deficiency promoted both NF-κB translocation in colonic tissues and the nuclear expression of p65 compared with DSS-treated BRD7$^{+/+}$ mice (Figure 6b). On the basis of these findings, we propose that BRD7 deficiency promotes pro-inflammatory effects by activating NF-κB in mice with DSS-induced early acute colitis.

DISCUSSION

Obvious evidence is available to support the hypothesis that inflammation promotes certain alterations within cells that are important to cancer advancement,[23] and many inflammatory signaling pathways are activated in several types of cancers, which links inflammation to the tumorigenesis process.[24] Moreover, diverse inflammatory mediators collectively act to create a favorable microenvironment for tumorigenesis.[25] BRD7 has been identified as a member of the bromodomain protein family[8] and as a tumor suppressor that is involved in cancer cell cycle progression and apoptosis initiation.[9] However, its role in inflammation has not been reported to date.

In the current study, we established a BRD7$^{-/-}$ mouse model and demonstrated that the BRD7$^{-/-}$ mice were more susceptible to inflammation compared with BRD7$^{+/+}$ mice (Figure 1). Increasing evidence suggests that tumor suppressors are closely related to inflammation. The programmed cell death protein 4 (PDCD4) protein acts as a tumor suppressor and has a critical role in maintaining the balance between inflammation and tumorigenesis.[26] PDCD4 promoted the activation of the transcription factor nuclear factor kappa-B (NF-κB) and suppressed expression of the anti-inflammatory cytokine IL-10 after an apoptotic or inflammatory stimulus.[27] BRD2, as a member of the bromodomain family, caused transcriptional downregulation of the NF-kB subunit p105/p50 and decreased the inflammatory response in human melanomas.[28] Infecting macrophages with the intracellular bacterial pathogen *Listeria monocytogenes* caused binding of the bromodomain and extra-terminal motif proteins BRD2 and BRD3.[29] Therefore, it is not surprising that BRD7, a member of the bromodomain family and a tumor suppressor, has a protective role in inflammation.

Bacterial LPS is a constituent of the outer membrane of the cell walls of Gram-negative bacteria with endotoxic activity. LPS can be recognized by epithelial cells, fibroblasts and macrophages via their surface CD14/TLR4 receptor complexes, resulting in the biological changes known as inflammation.[30] MEF cells are a valuable system for studying the cellular phenotype of genetically modified mice.[31] Therefore, we used LPS-induced acute inflammation in MEF cells from BRD7$^{-/-}$ and BRD7$^{+/+}$ mouse embryos and found that some of the classic inflammatory mediators, such as IL-6, TNF-α, CXCL-1 and iNOS, were significantly increased in BRD7$^{-/-}$ MEF cells compared with those in the BRD7$^{+/+}$ controls after the stimulation with LPS (Figures 2a–d), which suggests that BRD7 exerts anti-inflammatory effects by inhibiting the pro-inflammatory cytokines. Unexpectedly, the expression level of the anti-inflammatory factor IL-10 was also higher in BRD7$^{-/-}$ MEF cells than in the BRD7$^{+/+}$ controls (Figure 2e), which may have resulted from an inflammation-induced compensatory increase in anti-inflammatory factors or the reciprocal regulation of pro-inflammatory cytokines and anti-inflammatory factors. Previous studies have also illuminated that

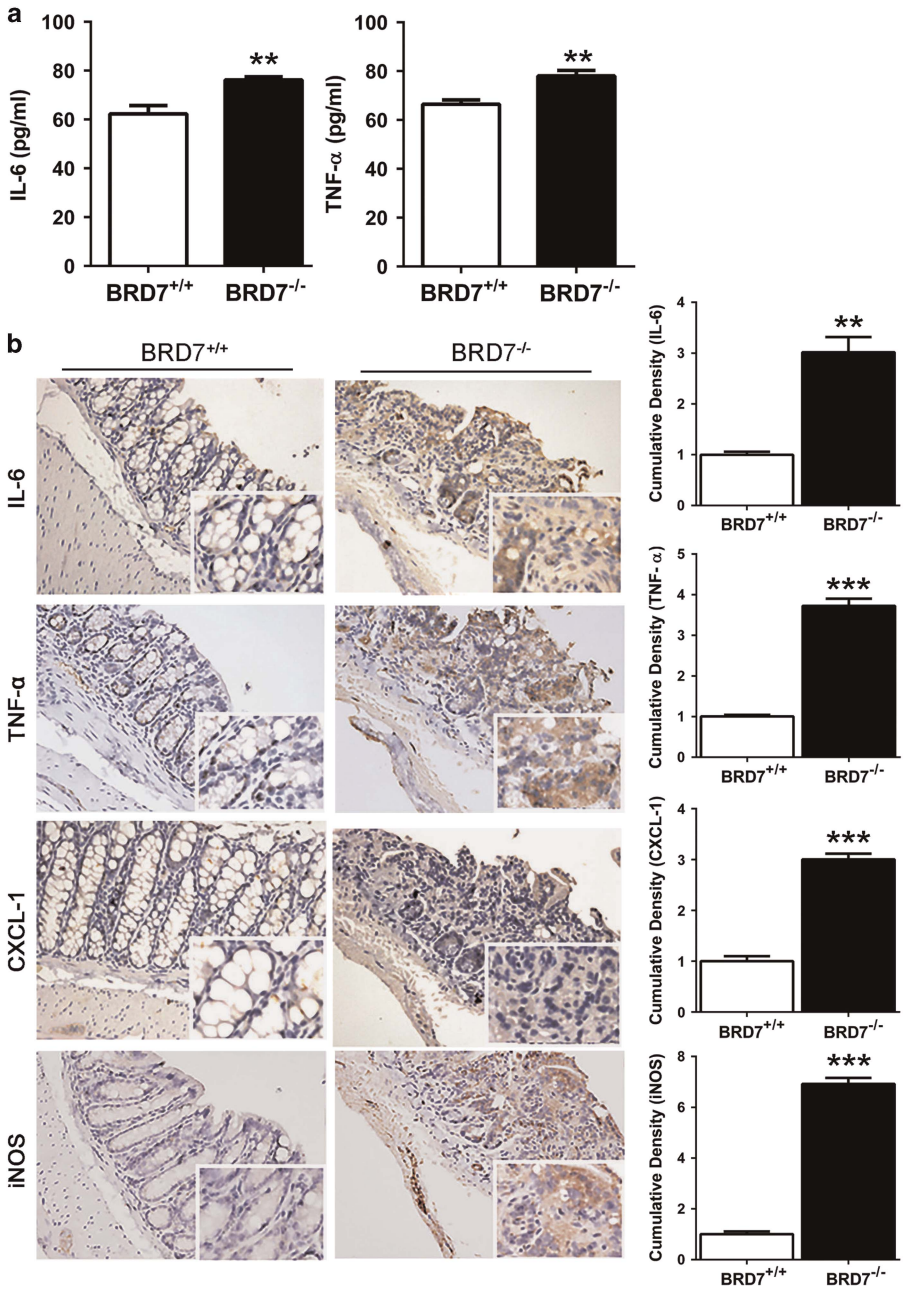

Figure 5 BRD7 deficiency promotes the production of inflammatory mediators in DSS-induced early acute colitis. (**a**) The expression and secretion of the inflammatory markers IL-6 and TNF-α were evaluated in the peritoneal fluid by ELISA. (**b**) The levels of IL-6, iNOS, CXCL-1 and TNF-α expression in the colon tissue were assessed by immunohistochemistry (×200 magnification). Right: summarized results. The results are representative of three independent experiments and are expressed as the mean values ± s.d. $^{**}P<0.01$, $^{***}P<0.001$ compared with the BRD7$^{+/+}$ mice with DSS-treated colitis. BRD7, bromodomain-containing protein 7; DSS, dextran sodium sulfate; ELISA, enzyme-linked immunoassay.

epratuzumab inhibited the production of the pro-inflammatory cytokines IL-6 and TNF-α but not the anti-inflammatory cytokine IL-10 in B cells derived from healthy donors and systemic lupus erythematosus patients,[32] and that the levels of both the pro-inflammatory cytokine IL-6 and the anti-inflammatory cytokine IL-10 increased postoperatively and peaked 1 day after using lymphokine-activated killer cells in patients with esophageal cancer.[33] IL-27 treatment rescued the Oncostatin M (OSM)-stimulated neurotoxicity by suppressing OSM-mediated TNF-α and iNOS expression by inactivating the NF-kB pathway.[34] Therefore, BRD7 deficiency exerts pro-inflammatory effects by promoting the expression and secretion of certain critical pro-inflammatory cytokines.

NF-kB, which is a transcription factor, has an important role in immune and inflammatory responses,[35–38] and its dysregulation has been associated with a number of inflammation-

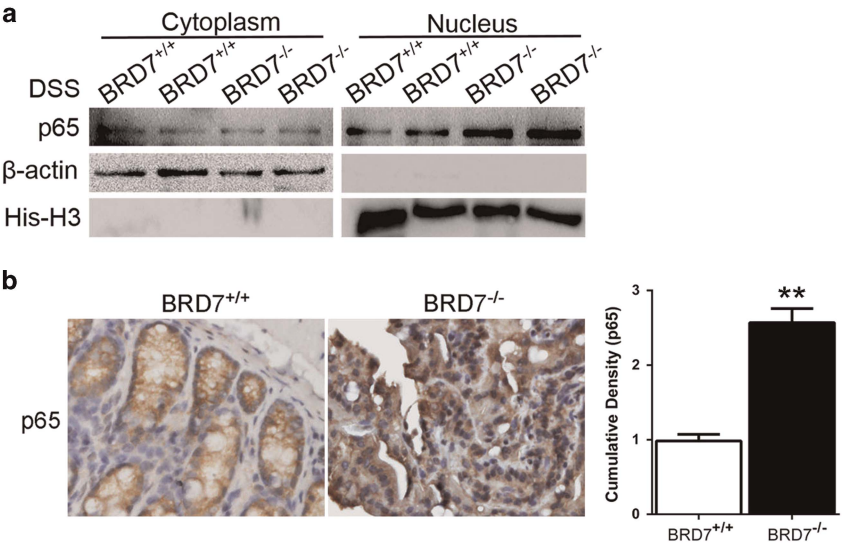

Figure 6 BRD7 exerts its anti-inflammatory activity via inhibition of NF-κB activation *in vivo*. (**a**) The protein expression of p65 in nuclear and cytoplasmic fractions of colonic tissues was examined by western blotting at 4 days following DSS treatment. (**b**) The protein expression of p65 in colonic tissues was assessed by immunohistochemical analysis (left, ×200 magnification). Right: graphical results. The results are representative of three independent experiments and are expressed as the mean values ± s.d. Differences between the groups were determined using ANOVA ($n=6$). $^{**}P<0.01$ compared with the BRD7$^{+/+}$ mice with DSS-induced colitis. ANOVA, analysis of variance; BRD7, bromodomain-containing protein 7; DSS, dextran sodium sulfate; NF-kB, nuclear factor kappa-B.

related diseases or disorders, including sepsis and septic shock,[39] cardiovascular disease, asthma, atherosclerosis, diabetes, obesity and cancer.[40–42] IL-6, TNF-α, CXCL-1 and iNOS are regulated through the NF-kB pathway.[43] In our study, an increased level of NF-kB activation was observed in BRD7$^{-/-}$ MEF cells after LPS stimulation for 1 h but recovered at the 6-h time point (Figure 3). Furthermore, the recovery of BRD7 expression reversed the inflammatory phenotype in BRD7$^{-/-}$ MEF cells (Figure 3e). These results demonstrate that BRD7 has a critical role in the early phase of acute inflammation by inhibiting the expression of NF-kB-regulated pro-inflammatory mediators.

The DSS-induced acute colitis mouse model has been used to elucidate mechanisms and to test therapeutic agents for colitis. We studied previous reports to determine the method for inducing this colitis model[44–46] and the approximate range of peptide dosage.[47–50] Consistent with the findings obtained using the LPS-induced MEF cells, BRD7$^{-/-}$ mice treated with DSS showed a progressively increased DAI, shorter colons and larger spleens compared with the BRD7$^{+/+}$ controls, even though no significant difference was detected in the late phase of acute inflammation (Figure 4). The main reason for this might be that the BRD7 deficiency has a pro-inflammatory role during the early stage of acute inflammation, whether in LPS-induced MEF cells or in DSS-induced mice, whereas compensatory expression of other critical genes in the late stage replaces the function of BRD7 and leads to a partial recovery of the inflammatory phenotype. Colitis is a nonspecific inflammatory disorder primarily involving the mucosa and submucosa of the colon, in which increased levels of pro-inflammatory mediators lead to an inflammatory cascade and tissue damage.[51] IL-6 is produced by various types of cells and exerts pleiotropic effects on various organ systems. Alterations in the level of production of IL-6 have been found in inflammatory states such as rheumatoid arthritis.[52] IL-6 stimulates neutrophilic chemotaxis and leads to tissue destruction in the colon. TNF-α, which is a pleiotropic cytokine, has a fundamental role in inflammatory disorders, such as colitis, by triggering the accumulation and activation of leukocytes.[53] Therefore, TNF-α is an important therapeutic target, and several engineered antibodies directed against TNF-α are beneficial for the treatment of inflammatory bowel syndrome.[54] In the present study, the levels of IL-6 and TNF-α secretion were elevated in the peritoneal fluid from DSS-induced BRD7$^{-/-}$ colitis mice. Similarly, the levels of IL-6, TNF-α, CXCL-1 and iNOS expression were increased in BRD7$^{-/-}$ colitis tissues, accompanied by the observable nuclear localization of NF-kB (p65). All of these findings suggest that BRD7 has a protective role in DSS-induced early acute colitis.

In summary, to investigate the function and underlying mechanism of action of BRD7 in inflammation, we constructed LPS-stimulated MEF cells, a BRD7 knockout mouse model and a DSS-induced acute inflammation model, and found that both the mice and MEF cells deficient in BRD7 were more susceptible to inflammation and that the expression and secretion of IL-6, TNF-α, CXCL-1 and iNOS were significantly increased after treatment with LPS or DSS, followed by obvious NF-κB (p65) nuclear translocation and NF-κB pathway activation during the early phase of acute inflammation. These findings suggest that the anti-inflammatory properties of BRD7 may result from the inhibition of IL-6, TNF-α, CXCL-1 and iNOS expression by preventing activation of the NF-κB pathway during early acute inflammation, which provides evidence for the therapeutic utility of BRD7 in inflammatory diseases.

CONFLICT OF INTEREST

The authors declare no conflict of interest.

ACKNOWLEDGEMENTS

This work was supported by grants from the National Natural Science Foundation of China (grant nos 81071686, 81328019 and 81572748) and the Free Exploration Program of Central South University (grant no. 2015zzts097). We thank the Shanghai Research Center for Biomodel Organisms (Shanghai, China) for their excellent technical assistance in generating the BRD7$^{-/-}$ mice.

1 Peng C, Liu HY, Zhou M, Zhang LM, Li XL, Shen SR *et al.* BRD7 suppresses the growth of nasopharyngeal carcinoma cells (HNE1) through negatively regulating beta-catenin and ERK pathways. *Mol Cell Biochem* 2007; **303**: 141–149.
2 Zhou J, Ma J, Zhang BC, Li XL, Shen SR, Zhu SG *et al.* BRD7, a novel bromodomain gene, inhibits G1-S progression by transcriptionally regulating some important molecules involved in ras/MEK/ERK and Rb/E2F pathways. *J Cell Physiol* 2004; **200**: 89–98.
3 Hu K, Liao D, Wu W, Han AJ, Shi HJ, Wang F *et al.* Targeting the anaphase-promoting complex/cyclosome (APC/C)- bromodomain containing 7 (BRD7) pathway for human osteosarcoma. *Oncotarget* 2014; **5**: 3088–3100.
4 Park YA, Lee JW, Kim HS, Lee YY, Kim TJ, Choi CH *et al.* Tumor suppressive effects of bromodomain-containing protein 7 (BRD7) in epithelial ovarian carcinoma. *Clin Cancer Res* 2014; **20**: 565–575.
5 Zhou M, Peng C, Nie XM, Zhang BC, Zhu SG, Yu Y *et al.* [Expression of BRD7-interacting proteins,BRD2 and BRD3, in nasopharyngeal carcinoma tissues]. *Ai Zheng* 2003; **22**: 123–127.
6 Berkovits BD, Wang L, Guarnieri P, Wolgemuth DJ. The testis-specific double bromodomain-containing protein BRDT forms a complex with multiple spliceosome components and is required for mRNA splicing and 3′-UTR truncation in round spermatids. *Nucleic Acids Res* 2012; **40**: 7162–7175.
7 Picaud S, Strocchia M, Terracciano S, Lauro G, Mendez J, Daniels DL *et al.* 9H-purine scaffold reveals induced-fit pocket plasticity of the BRD9 bromodomain. *J Med Chem* 2015; **58**: 2718–2736.
8 Sun H, Liu J, Zhang J, Shen W, Huang H, Xu C *et al.* Solution structure of BRD7 bromodomain and its interaction with acetylated peptides from histone H3 and H4. *Biochem Biophys Res Commun* 2007; **358**: 435–441.
9 Zhou M, Liu H, Xu X, Zhou H, Li X, Peng C *et al.* Identification of nuclear localization signal that governs nuclear import of BRD7 and its essential roles in inhibiting cell cycle progression. *J Cell Biochem* 2006; **98**: 920–930.
10 Kaeser MD, Aslanian A, Dong MQ, Yates JR, Emerson BM. BRD7, a novel PBAF-specific SWI/SNF subunit, is required for target gene activation and repression in embryonic stem cells. *J Biol Chem* 2008; **283**: 32254–32263.
11 Hugo HJ, Saunders C, Ramsay RG, Thompson EW. New insights on COX-2 in chronic inflammation driving breast cancer growth and metastasis. *J Mammary Gland Biol Neoplasia* 2015; e-pub ahead of print 21 July 2015; doi:10.1007/s10911-015-9333-4.
12 Ma X, Aoki T, Tsuruyama T, Narumiya S. Definition of prostaglandin E2-EP2 Signals in the colon tumor microenvironment that amplify inflammation and tumor growth. *Cancer Res* 2015; **75**: 2822–2832.
13 Fernandes JV, Cobucci RN, Jatoba CA, de Medeiros FT, de Azevedo JW, de Araujo JM. The role of the mediators of inflammation in cancer development. *Pathol Oncol Res* 2015; **21**: 527–534.
14 Dong ZW, Ren CG, Xia Y, Su D, Du TT, Fan HB *et al.* Pten regulates homeostasis and inflammation-induced migration of myelocytes in zebrafish. *J Hematol Oncol* 2014; **7**: 17.
15 Cooks T, Harris CC, Oren M. Caught in the cross fire: p53 in inflammation. *Carcinogenesis* 2014; **35**: 1680–1690.
16 Schmid T, Bajer MM, Blees JS, Eifler LK, Milke L, Rubsamen D *et al.* Inflammation-induced loss of Pdcd4 is mediated by phosphorylation-dependent degradation. *Carcinogenesis* 2011; **32**: 1427–1433.
17 Xu Y, Cao W, Zhou M, Li C, Luo Y, Wang H *et al.* Inactivation of BRD7 results in impaired cognitive behavior and reduced synaptic plasticity of the medial prefrontal cortex. *Behav Brain Res* 2015; **286**: 1–10.
18 Wang H, Zhao R, Guo C, Jiang S, Yang J, Xu Y *et al.* Knockout of BRD7 results in impaired spermatogenesis and male infertility. *Sci Rep* 2016; **6**: 21776.
19 Tominaga K, Kirikae T, Nakano M. Lipopolysaccharide (LPS)-induced IL-6 production by embryonic fibroblasts isolated and cloned from LPS-responsive and LPS-hyporesponsive mice. *Mol Immunol* 1997; **34**: 1147–1156.
20 Ren T, Tian T, Feng X, Ye S, Wang H, Wu W *et al.* An adenosine A3 receptor agonist inhibits DSS-induced colitis in mice through modulation of the NF-kappaB signaling pathway. *Sci Rep* 2015; **5**: 9047.
21 Wirtz S, Neufert C, Weigmann B, Neurath MF. Chemically induced mouse models of intestinal inflammation. *Nat Protoc* 2007; **2**: 541–546.
22 Cooper HS, Murthy SN, Shah RS, Sedergran DJ. Clinicopathologic study of dextran sulfate sodium experimental murine colitis. *Lab Invest* 1993; **69**: 238–249.
23 Rani P, Pal D, Hegde RR, Hashim SR. Acetamides: chemotherapeutic agents for inflammation-associated cancers. *J Chemother* 2015; e-pub ahead of print 21 July 2015; doi:10.1179/1973947815Y.0000000060.
24 Mao F, Wang M, Wang J, Xu WR. The role of 15-LOX-1 in colitis and colitis-associated colorectal cancer. *Inflamm Res* 2015; **64**: 661–669.
25 Fernandes JV, Cobucci RN, Jatoba CA, de Medeiros FT, de Azevedo JW, de Araujo JM. The role of the mediators of inflammation in cancer development. *Pathol Oncol Res* 2015; **21**: 527–534.
26 Jiang Y, Gao Q, Wang L, Guo C, Zhu F, Wang B *et al.* Deficiency of programmed cell death 4 results in increased IL-10 expression by macrophages and thereby attenuates atherosclerosis in hyperlipidemic mice. *Cell Mol Immunol* 2015; e-pub ahead of print 13 July 2015; doi:10.1038/cmi.2015.47.
27 Hilliard A, Hilliard B, Zheng SJ, Sun H, Miwa T, Song W *et al.* Translational regulation of autoimmune inflammation and lymphoma genesis by programmed cell death 4. *J Immunol* 2006; **177**: 8095–8102.
28 Gallagher SJ, Mijatov B, Gunatilake D, Gowrishankar K, Tiffen J, James W *et al.* Control of NF-kB activity in human melanoma by bromodomain and extra-terminal protein inhibitor I-BET151. *Pigment Cell Melanoma Res* 2014; **27**: 1126–1137.
29 Wienerroither S, Rauch I, Rosebrock F, Jamieson AM, Bradner J, Muhar M *et al.* Regulation of NO synthesis, local inflammation, and innate immunity to pathogens by BET family proteins. *Mol Cell Biol* 2014; **34**: 415–427.
30 Park BS, Song DH, Kim HM, Choi BS, Lee H, Lee JO. The structural basis of lipopolysaccharide recognition by the TLR4-MD-2 complex. *Nature* 2009; **458**: 1191–1195.
31 Sun H, Gulbagci NT, Taneja R. Analysis of growth properties and cell cycle regulation using mouse embryonic fibroblast cells. *Methods Mol Biol* 2007; **383**: 311–319.
32 Fleischer V, Sieber J, Fleischer SJ, Shock A, Heine G, Daridon C *et al.* Epratuzumab inhibits the production of the proinflammatory cytokines IL-6 and TNF-alpha, but not the regulatory cytokine IL-10, by B cells from healthy donors and SLE patients. *Arthritis Res Ther* 2015; **17**: 185.
33 Yamaguchi Y, Hihara J, Hironaka K, Ohshita A, Okita R, Okawaki M *et al.* Postoperative immunosuppression cascade and immunotherapy using lymphokine-activated killer cells for patients with esophageal cancer: possible application for compensatory anti-inflammatory response syndrome. *Oncol Rep* 2006; **15**: 895–901.
34 Baker BJ, Park KW, Qin H, Ma X, Benveniste EN. IL-27 inhibits OSM-mediated TNF-alpha and iNOS gene expression in microglia. *Glia* 2010; **58**: 1082–1093.
35 Lu W, Xu Y, Shao X, Gao F, Li Y, Hu J *et al.* Uric acid produces an inflammatory response through activation of NF-kappaB in the hypothalamus: implications for the pathogenesis of metabolic disorders. *Sci Rep* 2015; **5**: 12144.
36 Schuliga M. NF-kappaB signaling in chronic inflammatory airway disease. *Biomolecules* 2015; **5**: 1266–1283.

37 Berdyshev AG, Kosiakova HV, Onopchenko OV, Panchuk RR, Stoika RS, Hula NM. N-Stearoylethanolamine suppresses the pro-inflammatory cytokines production by inhibition of NF-kappaB translocation. *Prostaglandins Other Lipid Mediat* 2015; **121**: 91–96.
38 Jian CX, Li MZ, Zheng WY, He Y, Ren Y, Wu ZM *et al.* Tormentic acid inhibits LPS-induced inflammatory response in human gingival fibroblasts via inhibition of TLR4-mediated NF-kappaB and MAPK signalling pathway. *Arch Oral Biol* 2015; **60**: 1327–1332.
39 Russell JA. Management of sepsis. *N Engl J Med* 2006; **355**: 1699–1713.
40 Collins T, Cybulsky MI. NF-kappaB: pivotal mediator or innocent bystander in atherogenesis? *J Clin Invest* 2001; **107**: 255–264.
41 Chen F. Is NF-kappaB a culprit in type 2 diabetes? *Biochem Biophys Res Commun* 2005; **332**: 1–3.
42 Karin M, Cao Y, Greten FR, Li ZW. NF-kappaB in cancer: from innocent bystander to major culprit. *Nat Rev Cancer* 2002; **2**: 301–310.
43 Zhang DK, Cheng LN, Huang XL, Shi W, Xiang JY, Gan HT. Tetrandrine ameliorates dextran-sulfate-sodium-induced colitis in mice through inhibition of nuclear factor -kappaB activation. *Int J Colorectal Dis* 2009; **24**: 5–12.
44 Tai EK, Wu WK, Wong HP, Lam EK, Yu L, Cho CH. A new role for cathelicidin in ulcerative colitis in mice. *Exp Biol Med (Maywood)* 2007; **232**: 799–808.
45 Vieira EL, Leonel AJ, Sad AP, Beltrao NR, Costa TF, Ferreira TM *et al.* Oral administration of sodium butyrate attenuates inflammation and mucosal lesion in experimental acute ulcerative colitis. *J Nutr Biochem* 2012; **23**: 430–436.
46 Koon HW, Shih DQ, Chen J, Bakirtzi K, Hing TC, Law I *et al.* Cathelicidin signaling via the Toll-like receptor protects against colitis in mice. *Gastroenterology* 2011; **141**: 1852–63.e1-3.
47 Zhang H, Porro G, Orzech N, Mullen B, Liu M, Slutsky AS. Neutrophil defensins mediate acute inflammatory response and lung dysfunction in dose-related fashion. *Am J Physiol Lung Cell Mol Physiol* 2001; **280**: L947–L954.
48 Jiang Y, Yang D, Li W, Wang B, Jiang Z, Li M. Antiviral activity of recombinant mouse beta-defensin 3 against influenza A virus *in vitro* and *in vivo*. *Antivir Chem Chemother* 2012; **22**: 255–262.
49 Rivas-Santiago B, Rivas SC, Castaneda-Delgado JE, Leon-Contreras JC, Hancock RE, Hernandez-Pando R. Activity of LL-37, CRAMP and antimicrobial peptide-derived compounds E2, E6 and CP26 against Mycobacterium tuberculosis. *Int J Antimicrob Agents* 2013; **41**: 143–148.
50 Schlusselhuber M, Torelli R, Martini C, Leippe M, Cattoir V, Leclercq R *et al.* The equine antimicrobial peptide eCATH1 is effective against the facultative intracellular pathogen Rhodococcus equi in mice. *Antimicrob Agents Chemother* 2013; **57**: 4615–4621.
51 Hibi T, Inoue N, Ogata H, Naganuma M. Introduction and overview: recent advances in the immunotherapy of inflammatory bowel disease. *J Gastroenterol* 2003; **38**(Suppl 15): 36–42.
52 Polgar A, Brozik M, Toth S, Holub M, Hegyi K, Kadar A *et al.* Soluble interleukin-6 receptor in plasma and in lymphocyte culture supernatants of healthy individuals and patients with systemic lupus erythematosus and rheumatoid arthritis. *Med Sci Monit* 2000; **6**: 13–18.
53 van Deventer SJ. [Immunology in medical practice. IV. Inflammatory bowel diseases: pathogenic starting points for specific therapy]. *Ned Tijdschr Geneeskd* 1997; **141**: 1956–1959.
54 Hyams JS, Lerer T, Griffiths A, Pfefferkorn M, Kugathasan S, Evans J *et al.* Long-term outcome of maintenance infliximab therapy in children with Crohn's disease. *Inflamm Bowel Dis* 2009; **15**: 816–822.

Supplementary Information for this article can be found on the *Cellular & Molecular Immunology* website (http://www.nature.com/cmi)